Gray, D., Thornton, J. and Le Kernec, J. (2023) Small Boat Retro-reflectors. In: International Conference on Radar Systems (RADAR 2022), Edinburgh, UK, 24 - 27 October 2022, ISBN 9781839537776 (doi: 10.1049/icp.2022.2331)

There may be differences between this version and the published version. You are advised to consult the published version if you wish to cite from it.

http://eprints.gla.ac.uk/274250/

Deposited on 1 July 2022

Enlighten – Research publications by members of the University of Glasgow
http://eprints.gla.ac.uk

SMALL BOAT RETRO-REFLECTORS

Derek Gray[1], John Thornton[2], Julien Le Kernec[1*]

[1]James Watt School of Engineering, University of Glasgow, Glasgow, UK
[2]Antennas Research Ltd., York, UK
**Julien.LeKernec@glasgow.ac.uk*

Keywords: RCS, RADAR TARGET ENHANCER, CORNER REFLECTOR, SPHERICAL LENS

Abstract

Arrays of 8 trihedral corner-reflectors and arrays of 3 spherical lens retro reflectors were assessed against the ISO standard for 9.41 GHz maritime passive RCS enhancers. The trihedral array gave coverage for a third of the horizontal plane. In contrast an array of three ε_r=2.3 homogeneous spherical lenses with optimised air gap between lens and reflector cap gave full horizontal plane coverage above the RCS requirement as a low cost alternative to the Luneburg lenses presently in the market.

1 Introduction

Retro-reflectors are used as radar calibration targets and target enhancers [1]. Luneburg lenses fitted with 140° reflective spherical caps are used as radar calibration targets, and are attached to airborne towed targets, remotely piloted vehicles and marine platforms to simulate different types of potential target vehicles at low cost. Arrays of 3 Luneburg lens reflectors are used on marine safety buoys for navigation safety marking port entrances, channels and reefs. A further marine safety application is enhancing the radar cross-section (RCS) of small marine vessels under 150 gross tonnage (GT) which are poor reflectors of radar signals [1-4]. This is a result of these vessels been small, sitting low in the water and the hull been made of low reflectivity glass fibre reinforced plastic or wood [4]. As an example of the consequences of this small radar signature problem, between 2003 and 2007, an average of 780 ships were damaged per year in Japanese territorial waters [4]. Approximately 40% of the damaged ships were fishing boats in the 5 to 20 GT range. As of 2008, only about 8% of small boats had any type of marine radar reflector installed. Thus there is a need for legal compulsion as well as low cost dependable marine radar retro-reflectors. Any such retro-reflectors should meet the ISO8729 standard requirements, Table 1 [5].

Table 1 ISO8729 passive marine retro-reflector standard requirements, from [5]

Quantity	Value	In alternate units
9.41 GHz X-band RCS	7.5 m^2	8.75 dBm^2
height above sea level	4 m	
detection range	5 NM	9.26 km

Ideally all the reflected energy from a Luneburg lens fitted with a reflective cap is in phase so the RCS is the same as that of a flat circular plate or disc [5, 6]. The theoretical RCS of a flat disc is calculated by (1).

$$\sigma = \frac{4\pi^3 r^4 \lambda_0^4}{\lambda_0^2} = 4\pi^3 r^4 \lambda_0^2 \quad (1)$$

where λ_0 is the free space wavelength and r is the radius in multiples of λ_0

As a result of the λ_0 dependency, scaling a retro-reflector to a new frequency will not give the same RCS. This work was done at 12 GHz instead of 9.41 GHz due to the availability of test equipment and reducing the weight of any prototypes. This necessitates modification of the ISO8729 RCS requirement. At 9.41 GHz, an RCS of 8.75 dBm^2 is returned by a $2.78\lambda_0$ radius flat disc. A $2.78\lambda_0$ radius flat disc at 12 GHz gives an RCS of 6.64 dBm^2, which is used here as "ISO8729 mod" [8]. As have a 100 mm radius lens from prior work, took $4\lambda_0$ radius as a standard size in this work for which the theoretical RCS of a flat disc is 12.98 dBm^2, which exceeds "ISO8729 mod" by 6.3 dB.

2. Corner-reflector baseline design

Approximately one in fifty small vessels harboured at marinas in the Kobe and Himeji area in early 2020 were equipped with an array of 8 square trihedral corner-reflectors (Figure 1). Thus, informally, the usage of RCS enhancers has not increased in 12 years. This low cost and low mass passive retro-reflector was made from 300 mm sided squares of marine grade aluminium, and is conveniently suspended from a bracket on a lighting mast or some other suitable high point of a boat. The array was simulated in FEKO™ using the Method of Moments (MoM) solver illuminated by a horizontally polarised plane wave at 9.41 GHz [9]. Across ±15° elevation to cover boat moderate pitch and roll, the ISO8729 specification was only met across 24° to 28° in each quadrant, giving 112° best case coverage which is about a third of the horizontal plane. Thus for two thirds of the horizon, this device gave an insufficient return, akin to the measured results from similar corner-reflector arrays in [1].

Figure 1. Photograph of an 8 corner-reflector on a small boat.

For direct comparison to the lens retro-reflectors at 12 GHz, the square side length was reduced to 200 mm matching the lens diameters. Each trihedral corner-reflector was thus composed of 100 mm sided square plates, and on axis (aligned with the X-axis here) was seen as a 163 mm diameter hexagon which theoretically would give 7.8 dBm^2 RCS exceeding "ISO8729 mod" by 1.1 dB [6].

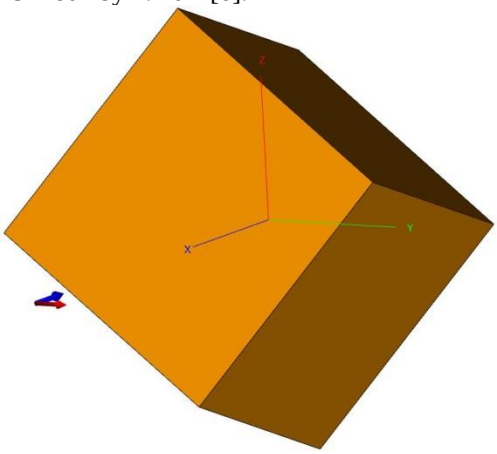

Figure 2. CAD of a single square trihedral corner-reflector.

The 100 mm sided single square trihedral corner-reflector was symmetrical about the horizontal XY-plane as per the actual device, Figures 1 and 2. As it was not rotationally symmetric about the vertical Z-axis, this necessitated rotation through the full 360° in FEKO™ simulation. Illumination was by a horizontally polarized plane wave incident along the X-axis, Figure 2. The peak RCS was 6 dBm^2 on axis with 33° 3dB coverage as shown in Figure 3. The sharp lobes at 124° and 305° were reflections from the vertical flat plate, and the 34° lobe from the dihedral plates.

The full 8 corner-reflector array was simulated in FEKO™ for 0° to 180° as the device was symmetrical about the YZ-plane when the front X was centred on the X-axis as shown in Figure 4. The monostatic RCS pattern shape was the same as found previously in [9] been a superposition of the single corner-reflector pattern with some ripple (see Figure 5). Thus in spite of the array always presenting a flat projected area larger than a 100 mm radius disc to the illuminating plane wave, it failed to meet "ISO8729 mod" except with the narrow lobes at 0° and 90°.

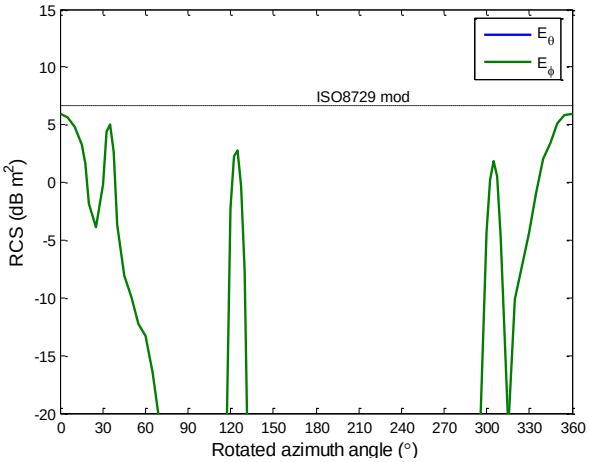

Figure 3. Monostatic RCS of the single square trihedral corner reflector at 12 GHz from FEKO™.

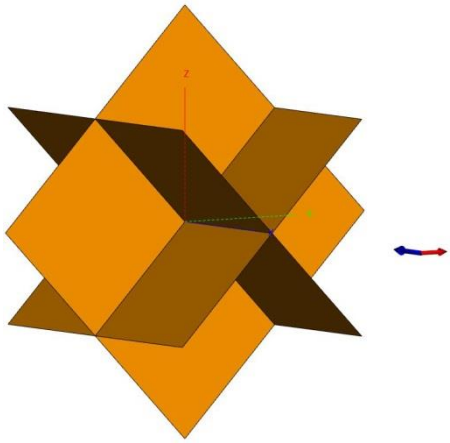

Figure 4. CAD of the 8-corner-reflector array.

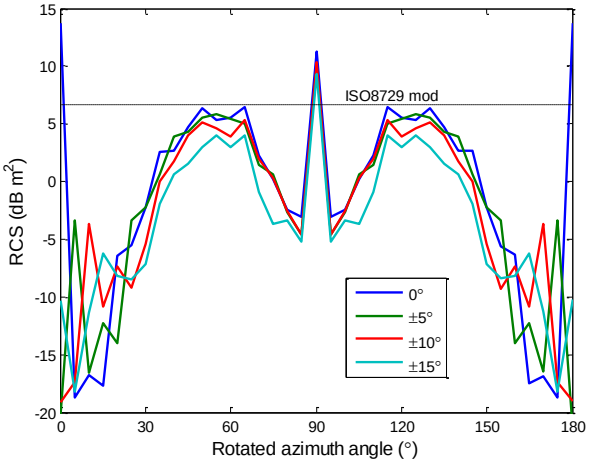

Figure 5. Monostatic RCS of the 8-corner reflector array at 12 GHz for different pitch/roll angles from FEKO™.

The bistatic radiation patterns of the array show that it did collect and reradiate sufficient power to satisfy "ISO8729 mod" but the power was reradiated away from the X-axis (Figure 6). This fundamental property of corner-reflectors cannot be changed so there is a need to develop a retro-reflector array element that reradiates at the illuminator irrespective of orientation.

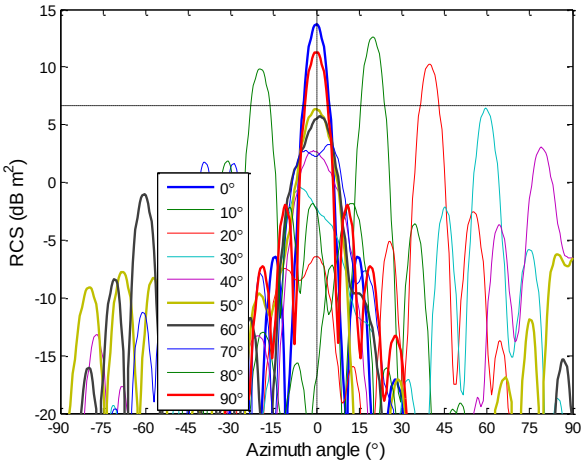

Figure 6. Bistatic RCS of the 8-corner reflector array for different rotated angles from FEKO™.

3 Homogeneous lens retro reflector

Commercially available Luneburg lenses with 140° arc angle reflective caps are used in 3-element arrays where each lens covers a 120° sector. The light weight of Luneburg lenses is attractive but the high cost of specialised high precision foam moulding is an economic barrier to wide spread adoption. It is understood that homogeneous spherical lens antennas give satisfactory performance for gains up to 30 dBi having radii in the 4 to 5λ_0 range [10], which matches the radius required to meet the ISO8729 specification. A homogeneous spherical lens retro-reflector such as Figure 7 is a feasible low cost array element.

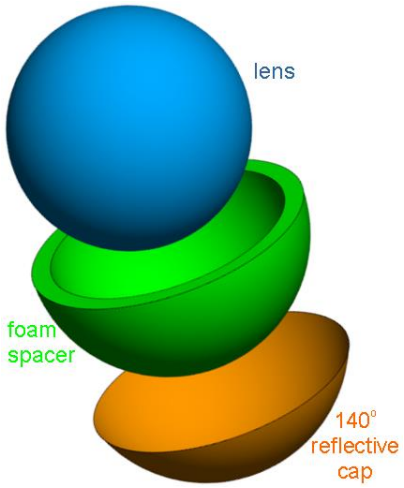

Figure 7. Exploded view of a spherical lens passive retro-reflector.

With the 140° reflective cap on the spherical lens surface (no air gap), 2λ_0, 3λ_0 and 4λ_0 radius spheres were simulated in FEKO™ for ε_r=2 to ε_r=4 (Figure 8). Interestingly, the 2λ_0 and 3λ_0 radii spheres both met or exceeded the theoretical RCS of a flat disc for ε_r=2.9 and some greater values. The general trend for all 3 radii was increasing RCS from ε_r=2 to ε_r=2.9 after which the RCS oscillated and decreased. The latter fits with the known increasing restriction of spherical lens aperture due to total internal reflection above ε_r=2.2 [11]. The RCS oscillations indicate the complexity of the combination of different mechanisms contributing to the reflected signal and suggest that there will be rapidly changing RCS with frequency. Reviewing prior work on backscatter from dielectric spheres elucidated the numerous reflection and transmission paths [12, 13] (Figure 9). Evidently the various reflections added for the super-directivity state of the 2λ_0 radius ε_r=2.9 lens. Resolving the different components adding or subtracting will require careful study with a time domain solver.

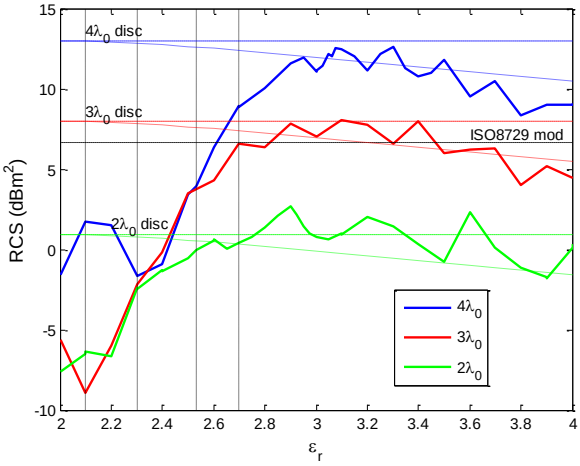

Figure 8. RCS variation with ε_r for 2λ_0, 3λ_0, and 4λ_0 radii lenses with 140° reflective cap and no air gap compared to equal radii flat discs; from FEKO™.

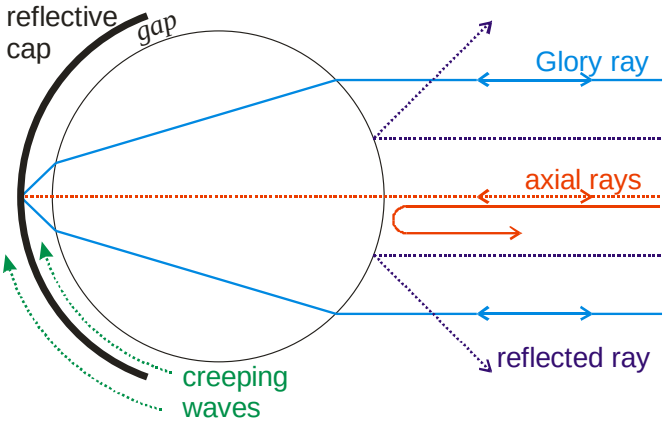

Figure 9. Reflection mechanisms in a spherical homogeneous lens passive retro-reflector.

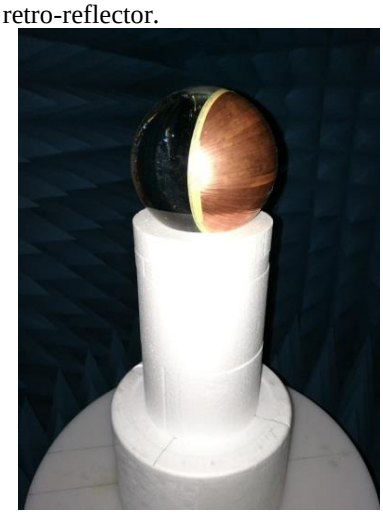

Figure 10. 75 mm radius crystal ball under test.

A 75 mm radius crystal ball was purchased and copper tape strips were applied to form a 140° reflective cap (Figure 10). The device was mounted atop a Styrofoam column on the rotator in an anechoic chamber and measured across 11 to 13 GHz. Both measured and simulated RCS showed rapid oscillations with frequency which would be a severe disadvantage to an operational retro-reflector in that small dimension manufacturing errors will significantly affect the performance by 6 dB. It is assumed that the glass had a high metal content and thus was highly lossy. The effect of any dielectric losses is unquantified but there was a 4.5 dB offset between measured RCS and simulation of ε_r=3.60 with no losses (Figure 11). For 11.4 to 12.6 GHz, the measured and simulated oscillation peaks coincided but the trend was different. The monostatic RCS patterns were relatively flat across ±60° and 10 to 15 dB above the rest of the pattern giving proof-of-concept (Figure 12).

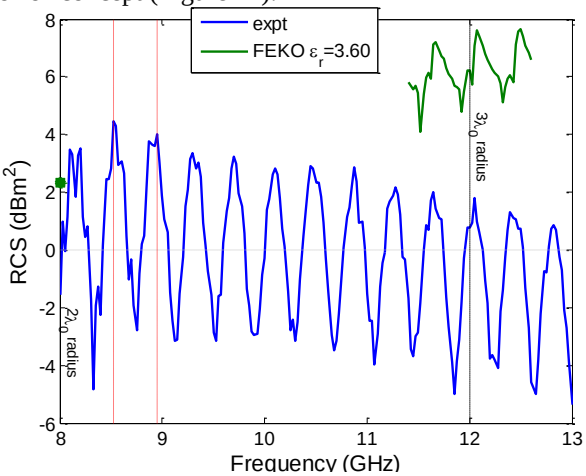

Figure 11. Measured RCS of the 75 mm radius crystal ball.

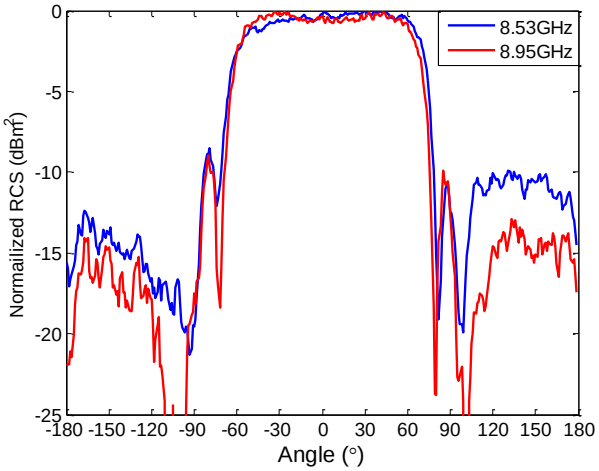

Figure 12. Measured monostatic patterns of the 75 mm radius crystal ball.

It was assumed that the dielectric surface waves on the spherical lens surface had lesser amplitude at lower ε_r and that the rate of change of the RCS oscillations with frequency would be less at lower ε_r. Thus common machinable plastics having ε_r in the 2.1 to 2.7 range were investigated. Plane wave illumination of different ε_r $4\lambda_0$ radius lenses showed that the focal zone became less diffuse and moved closer to the lens surface with increasing ε_r trending toward the ideal point on the lens surface at ε_r=3.60 glass [11] (Figure 13). The off-surface focal zones reflect off the spherical cap with both phase and amplitude error which decreases with increasing ε_r giving increasing RCS until $\varepsilon_r \approx 2.9$ above which the aperture restriction from internal reflection begins the downward trend seen in Figure 8. Consequently, the reflective cap must be off the lens surface to successfully reflect the focal zone.

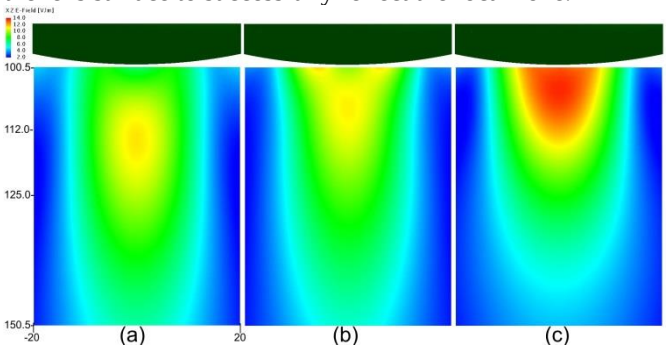

Figure 13. Electric near field of $4\lambda_0$ – 100 mm radius homogeneous lenses in response to plane wave illumination at 12 GHz from FEKO™ - (a) ε_r=2.10, (b) ε_r=2.30, (c) ε_r=2.54.

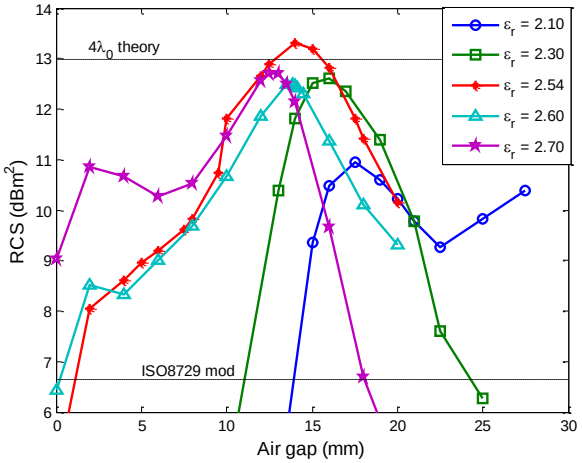

Figure 14. RCS variation with air gap between different ε_r $4\lambda_0$ radius spherical lenses and the reflective cap at 12 GHz from FEKO™.

The air gap was varied for $4\lambda_0$ radius spherical lenses having ε_r=2.1 to 2.7 at 12 GHz (Figure 14). The air gap for highest RCS decreased with increasing ε_r. There was no consistent trend in the highest RCS with increasing ε_r, once again suggesting complex interaction of the various reflections and transmission paths through and around the sphere with a reflective cap. The air gaps for highest RCS are summarised in Table 2. These designs were swept across 11.4 to 12.6 GHz, see Figure 15. The super-directivity state noted above occurred for every ε_r with the RCS exceeding that of an equal radius flat disc for a narrow band noted in Table 2. The monostatic pattern ranges of 0.8 to 1.6 dB across ±60° thus been suitable for sector coverage as shown in Figure 16 and Table 2. It was a happy accident that the ε_r=2.54 Rexolite lens had its super-directivity state at 12 GHz.

Table 2. Performance of different ε_r $4\lambda_0$ radius lenses

ε_r	Gap (mm)	Frequency (GHz)	RCS range (dB)
2.30	16.0	11.88	1.56
2.40	14.5	11.86	0.77
2.54	14.0	12.00	1.45
2.60	13.7	11.88	1.28
2.60	13.7	12.10	1.44
2.70	12.8	11.95	1.27

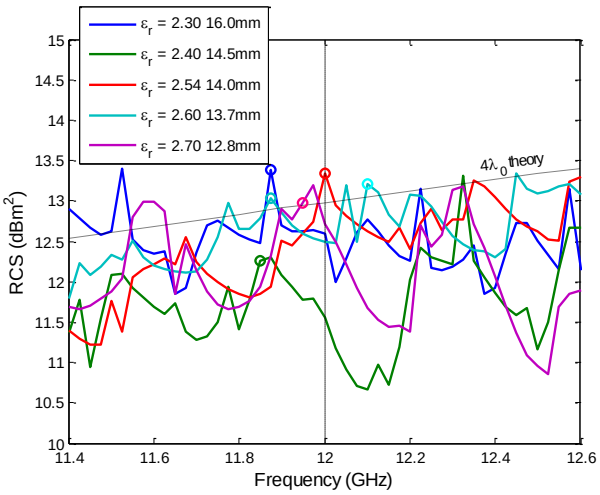

Figure 15. Frequency sweeps of different ε_r lenses with optimised air gap from FEKO™.

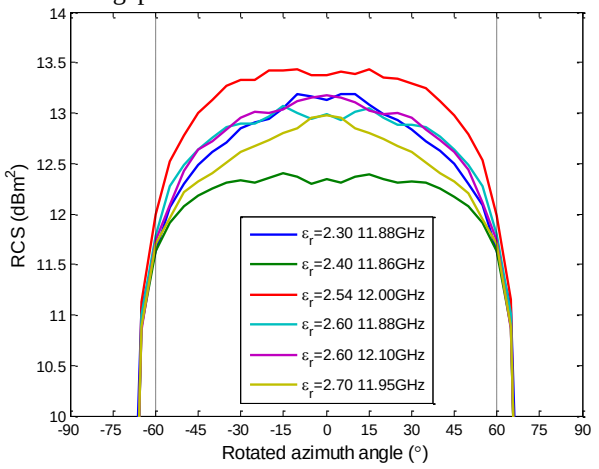

Figure 16. Monostatic scan patterns of super-directivity cases of Table 2 from FEKO™.

High Density Polyethylene (HDPE) and Ultra High Molecular Weight Polyethylene (UHMWPE) are available as large billets at low cost for ε_r=2.30, have low dielectric loss, and were used in the past for X-band antenna applications [10, 14]. Varying the air gap from 15 to 16 mm did not move the super-directivity state closest to 12 GHz (Figure 17). A Neader-Mead Simplex optimisation for both lens radius and air gap was run in FEKO™ to maximise RCS at 12 GHz. The optimal design had sphere radius of 98.95 mm with gap size of 15.94 mm. A frequency sweep from 11.4 to 12.6 GHz showed that this optimisation of both dimensions successfully moved the series of RCS peaks and troughs 120 MHz up in frequency, centring the super-directivity state on 12 GHz (Figure 17). HDPE has a specific gravity of 1, so a spherical lens will weigh 4kg which is not problematic on a small boat.

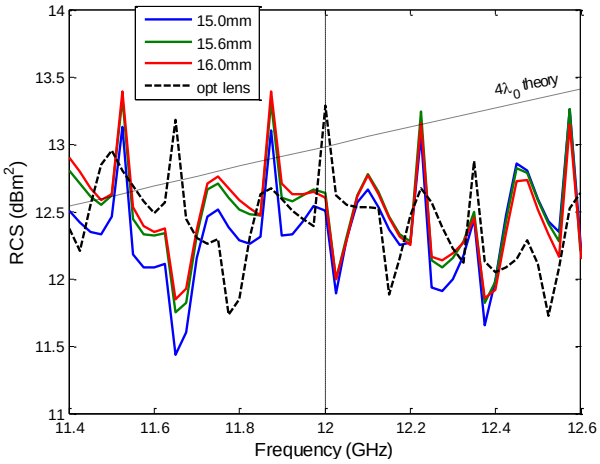

Figure 17. Frequency sweeps of ε_r=2.30 lens with different air gap sizes from FEKO™.

4 Homogeneous lens array

The optimised ε_r=2.30 98.95 mm radius lens was simulated in a 3-element array to give full 360° coverage in the horizontal plane as required by the ISO8729 specification as shown in Figure 18. Z-axis to lens centre spacings of 135mm and 150mm were run in FEKO™.

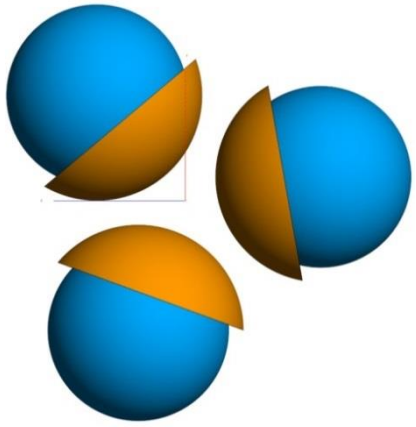

Figure 18. CAD of the 3-element ε_r=2.30 lenses from FEKO™.

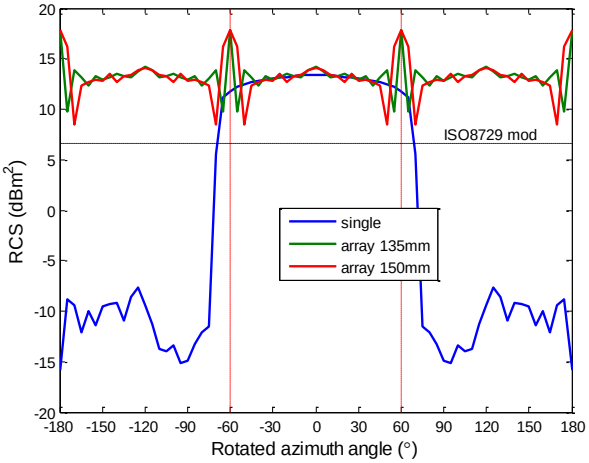

Figure 19. Monostatic RCS patterns of single and the 3-element arrays of ε_r=2.30 lenses from FEKO™.

The monostatic RCS patterns of the 3-element array successfully gave higher RCS than "ISO8729 mod" across the

full 360° horizontal plane (Figure 19). However, the RCS patterns were not a simple superposition of three single-lens patterns having discontinuities at the cross-overs that were dependent on array element spacing. This is presumed to be a circular array effect and will be studied in the future.
The bistatic RCS patterns of the 2 array spacings simulated had distinct mainlobe and first sidelobes for 0° rotation (Figure 20). The peak RCS of both arrays were close to equal but the first sidelobe levels differed. For 135 mm spacing the first sidelobe level was -16.7dB, been close to the -17.6dB below peak of an ideal circular aperture with uniform aperture distribution to produce maximum directivity. With 150 mm spacing the first sidelobe level increased by 2 dB showing reflection from the rear 2 array elements. The effect of lens spacing will be studied further and care will taken with mount design.

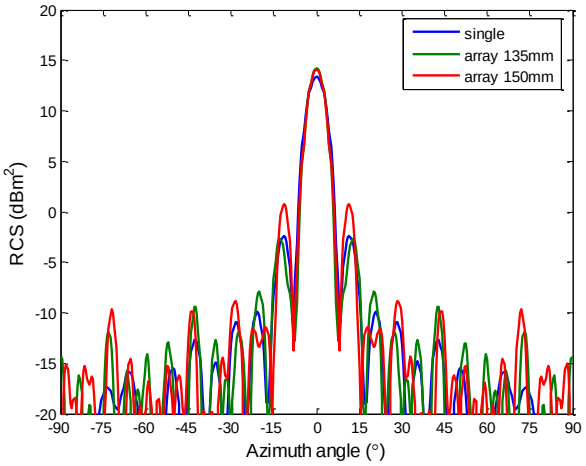

Figure 20. Bistatic RCS pattern for 0° azimuth rotation angle from FEKO™.

5 Conclusion

A common low-cost array of trihedral corner-reflectors was assessed and found to not meet the ISO8729 X-band marine retro-reflector standard. A homogeneous spherical lens that fits within the volume of the corner-reflector array was developed which met the standard across 120° of the horizontal plane. Correct sizing of the air gap between the spherical lens and its 140° spherical cap reflector was found to be critical for receiving and reradiating the power in the diffuse focus of the lens. A single polyethylene lens would weigh 4kg and was shown to be suitable for use in a 3-element array to give full horizontal plane coverage with 5 dB margin above the ISO8729 standard.

6 Acknowledgements

The authors wish to thank Dr. M. Ide of MOL Marine & Engineering Co., Ltd. for her advice, encouragement and enthusiasm.

7 References

[1] Luke, S.: 'Performance investigation of marine radar reflectors on the market', QinetiQ CR0704527, Mar. 2007.
[2] Yamada, T., Hayashi, S., Takenaka, Y.: 'Radar reflection characteristics of small glass-fiber reinforced plastic ship', Navigation, 2003, 155, pp. 67-70 (in Japanese).
[3] Heibatake, H., Hayashi, S., Ide, M.: 'A basic study on enhancement of electrical visualization for small boat', Asia Navigation Conf., Shanghai, Nov. 2008
[4] Ide, M., Hayashi, S.: 'Radar cross section for small fishing boats made of FRP', Navigation, 2009, 171, pp. 54-59 (in Japanese)
[5] Ships and marine technology - marine radar reflectors - part 1: passive type, ISO 8729-1 1st ed., 2010-01-15.
[6] Southworth, G.C.: 'Principals and applications of waveguide transmission' (D. van Nostrand Company, Inc., Princeton, NJ, 1950).
[7] Bird, D.: 'Design and manufacture of a low-profile radar retro-reflector', RTO SCI Symposium on Sensors and Sensor Denial by Camouflage, Concealment and Deception, Brussels, Belgium, 19-20 April 2004, RTO-MP-SCI-145.
[8] Gray, D.: 'Homogeneous spherical lens for marine retro-reflector application', IEICE Tech. Rep., Takamatsu, Japan, 119, (379), AP2019-178, Jan. 2020, pp. 153-158.
[9] Gray, D.: 'Homogeneous spherical lens for marine retro-reflector application, part 2', IEICE Tech. Rep., Hyogo University, Japan, 120, (135), AP2020-26, Aug. 2020, pp. 17-22.
[10] Gray, D., Thornton, J.: 'Scan performance of low index lens reflector', IET Int. Radar Conference, Xi'an, April 2013, paper G0470.
[11] Cheston, T.C., Luoma, E.J.: 'Constant-k lenses', APL Technical Digest, 2, (4), March-April 1963, pp. 8-11.
[12] Atlas, D., Glover, K.M.: 'Backscatter by dielectric spheres with and without metal caps', Proc. Inter-Disciplinary Conf. Electromagnetic Scattering, Potsdam, N.Y., Aug., 1962, Pergamon Press, New York, N.Y.
[13] Rheinstein, J.: 'Backscatter from spheres: a short pulse view', Lincoln Laboratory, MIT, Tech. Rep. 414, April 27, 1966.
[14] Thornton, J.: 'Wide-scanning multi-layer hemisphere lens antenna for Ka band," IEE Proc.-Microw. Antennas Propag., 153, (6), Dec. 2006, pp. 573-578.